Materials & Design 238 (2024) 112704

Contents lists available at ScienceDirect

Materials & Design

journal homepage: www.elsevier.com/locate/matdes

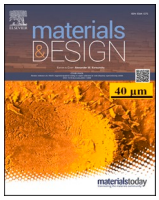

The design and manufacturing of a Patient-Specific wrist splint for rehabilitation of rheumatoid arthritis

Mo Zhou [a], Changning Sun [a,b], Seyed Ataollah Naghavi [a], Ling Wang [b], Maryam Tamaddon [a], Jinwu Wang [c], Chaozong Liu [a,*]

[a] Institute of Orthopaedic & Musculoskeletal Science, Division of Surgery & Interventional Science, University College London, Royal National Orthopaedic Hospital, Stanmore, London HA7 4LP, UK
[b] State Key Laboratory for Manufacturing Systems Engineering, School of Mechanical Engineering, Xi'an Jiaotong University, Xi'an, Shaanxi Province, China
[c] Shanghai Key Laboratory of Orthopaedic Implants, Department of Orthopaedic Surgery, Shanghai Ninth People's Hospital, Shanghai Jiao Tong University, Shanghai, China

ARTICLE INFO

Keywords:
Wrist splint
Finite element analysis
Topology optimisation
Rheumatoid arthritis

ABSTRACT

Wrist splint is a device for immobilising the wrist to facilitate the healing of wrist injury. However, conventional splint designing strategies lack consideration of biomechanical interaction with wrist joints, resulting in mechanical failure of splints or causing patient injuries. A novel design and optimisation method of customised functional wrist splints is needed clinically. In this study, we proposed a splint design method combining topology optimisation and additive manufacturing, based on the biomechanical analysis, to enable advanced customisation regarding functionality, comfort and ventilation. Three prototypes were fabricated via fused filament fabrication (FFF) horizontal printing, FFF vertical printing, and powder bed fusion (PBF). Finite element analysis was used to simulate the displacements of splints under the maximum loading provided by patients, with the results validated by physical tests. The stiffness and functionality of splints fabricated by different techniques were evaluated and compared. The results demonstrate that the developed splint is compatible with patients' functional and biomechanical needs, limiting 95.7% sagittal movement, 89.8% coronal movement, and 18.7% maximum grip strength. Moreover, among the three manufacturing methods, FFF vertical printing is recommended for general clinical use considering the safety, functionality, surface quality and cost.

1. Introduction

Rheumatoid arthritis (RA) is an autoimmune-mediated progressive inflammatory, with the wrist being one of the most commonly affected joints [1,2]. 50 % of patients experience wrist pain and swelling in the first two years, which increases to 90 % after ten years [3]. This suffering affects patients' daily activities and social life [4,5].

Functional wrist orthosis or splint, a recommended RA conservative treatment, is designed as an immobilisation device to provide support and stability for the wrist joint, preventing it from bending at "incorrect" angles [6–8]. Wearing splints is demonstrated to be beneficial in pain reduction and function improvement, preventing patients from secondary injuries [4,5,9].

In contrast to resting splints designed to immobilize the wrist during nighttime or at rest, functional splints are wearable in daily activities or occupational settings, providing support while ensuring hand functionality [10]. Therefore, an ideal RA functional wrist splint should be able to maintain the joint in a pain-relieving position with 10-15° extension and 5-10° ulnar excursion [11] while limiting grip as little as possible to retain hand function [12]. Besides, comfort, fit, and aesthetics, as important factors affecting patient compliance, should also be considered [13]. Pressure points, lack of ventilation, difficulty in cleaning, and the Velcro sticking to clothing are reasons why patients refuse to wear splints for extended periods [8].

However, existing wrist orthoses do not adequately meet patients' needs. One of the reasons is the limitations of the manufacturing method. Traditional functional splints are clinically fabricated using plaster (negative plaster cast, vacuum shaping, and trim shape) or low-temperature thermoplastic material (LTT) (cut and shaped directly on the hand) [14,15]. Both approaches require skilled technicians and are

* Corresponding author.
E-mail addresses: mo.zhou.20@ucl.ac.uk (M. Zhou), sun.cn@xjtu.edu.cn (C. Sun), seyed.naghavi.14@ucl.ac.uk (S.A. Naghavi), menlwang@mail.xjtu.edu.cn (L. Wang), m.tamadon@ucl.ac.uk (M. Tamaddon), wangjw-team@shsmu.edu.cn (J. Wang), chaozong.liu@ucl.ac.uk (C. Liu).

https://doi.org/10.1016/j.matdes.2024.112704
Received 21 November 2023; Received in revised form 19 January 2024; Accepted 24 January 2024
Available online 28 January 2024

associated with extended patient cooperation, which is not conducive to subsequent splint revision and replacement [14,15]. Traditional splints tend to have a uniform shape and lack of vents [15]. In addition, LTT braces are difficult to fit the skin due to their material properties, resulting in an ill-fitting interface that may cause local pressure sores, impede the healing process, and potentially harm the underlying tissue, exacerbating symptoms [16,17]. A similar situation occurs with commercial prefabricated splints, which have a worse fit and questionable efficacy [7,11,18].

Additive manufacturing (AM) offers a potential solution integrated with 3D scanning and computer-aided design (CAD), achieving advanced splint customization [15,19,20]. Compared to conventional processes, 3D scanning enables a quick collection of patient surface anatomical data without skin contact [21,22]. With the scanned data, CAD modelling can impart personalized complex structures to orthoses [30], including pocket creation [23] and multi-material design [13]. Furthermore, the manufacture of AM splints is based on digital models, facilitating batch production and replacement [24], benefiting patients with degenerative conditions (e.g. RA) requiring long-term splinting [25]. At present, AM has been widely applied in the fabrication of upper and lower limb orthoses as well as spinal orthotic devices [19,26–31].

The second reason for the unsatisfactory of existing splints stems from a lack of biomechanical considerations in their structural design. In current research and clinical practice, most orthotic devices rely on empirical-based design principles, especially in shape customization, thickness, skin breathing holes, and material increments or reductions [13,15,27,30,32–34]. This empirically driven approach amplifies the dependence on skilled technicians, and the dearth of mechanical accordance renders easier splint damage [26,27,30].

A viable approach is incorporating finite element analysis (FEA) into the splint processing [28]. FEA enables the simulation and evaluation of whether the digital models meet the desired mechanical performance, offering theoretical support for splint modifications [35,36]. Furthermore, in contrast to subjective or array-based pocket design [13,32,33,37], topology optimization (TO) based on FEA represents a superior choice [28] as TO allows for a reduction of the model's surface volume while preserving its original mechanical performance to the greatest extent possible [30].

However, research involving FEA and TO in AM splint design remains limited, primarily focusing on spinal and lower limb applications, such as the Boston brace [31], fracture stabilisation splints [29], or plaster casts [30]. Besides, TO was applied in several finger splints [26,27] and resting hand splints [28]. No research was found pertaining to the functional wrist splint design combined with AM and TO. Given the functional nature of these splints, a biomechanically based design is imperative. Hence, a clinically applicable orthoses design and manufacturing framework incorporating AM and TO is needed.

In this paper, we proposed a splint design strategy that combines topological optimization and additive manufacturing. Based on this strategy, three prototypes were fabricated using distinct manufacturing methods. The evaluation results illustrated how the designed splints meet the patients' needs. Furthermore, the most appropriate clinical manufacturing approach was identified, taking into account the splints' safety, functionality, surface quality, and cost. Besides wrist splints, this proposed design strategy and manufacturing methodology hold the potential for application in other additively manufactured orthotics and splints.

2. Materials and methods

2.1. Study design

The primary objectives of this study are as follows: 1) propose a splint design strategy; 2) based on the strategy, fabricate prototypes using distinct AM methods and evaluate their performance; 3) determine the most clinically suitable manufacturing approach.

The presented strategy is depicted in Fig. 1, with biomechanical FEA and TO providing theoretical support.

Three distinct splint prototypes were designed, manufactured and evaluated to verify the proposed strategy.

The design principles are predicated upon the following clinical requirements: 1) maintain the wrist joint at 10-15° extension and 5-10° ulnar deviation for pain relief [11]; 2) minimize the grip restriction to preserve hand function [12]; 3) consider comfort, fit, and aesthetics [13] to enhance patient compliance, avoiding pressure points, inadequate ventilation, difficult cleaning, and the Velcro sticking to clothing [8].

The fabrication strategy includes two clinically prevalent techniques: Fused Filament Fabrication (FFF) and Powder Bed Fusion (PBF) [13,32]. In FFF, thermoplastic materials are processed into filaments, heated, extruded through a nozzle, and deposited layer by layer on a printing platform [38]. In PBF, the principle is selective laser sintering of powdered materials, with the platform descending after each layer is sintered [39]. Besides, given the impact of deposition direction in FFF on product mechanical properties [38,40], this study employed two common deposition orientations: vertical printing and horizontal printing. Thus, the three manufacturing methods of the splint prototypes were: FFF horizontal printing (Z = frontal axis at anatomical position), FFF vertical printing (Z = vertical axis at anatomical position), and PBF printing.

Finally, splint performances were validated through FEA, three-point bending test, joint mobility assessment, grip strength evaluation, and hand function assessment.

2.2. Materials and properties

The designed splint used rigid and flexible materials. The hard part is designed for mechanical support, and the soft part is designed as comfortable edges and a linkage for easy donning and doffing. Following the consultation with orthotists, two rigid materials were selected: durable and biodegradable polylactic acid (PLA) for FFF processing [38,41] and nylon (polyamide-PA2200) with suitable elasticity and bending strength for PBF processing [6]. Besides, the bendable acrylic-based resin (50 shores) was chosen for the soft part. Fig. 2 shows in detail the material selection for the different parts of the splint.

Material properties were obtained from manufacturers (Table 1). Given the anisotropy in Z-axis (deposition direction) in FFF products [38,42], the elastic modulus of PLA was experimentally determined.

PLA standard samples for tensile (150 × 10 × 4 mm3) and three-point bending (80 × 10 × 4 mm3) tests were created according to ISO 527–4 and ISO 178 guidelines, respectively. SOLIDWORKS 2021 (Dassault Systèmes, Vélizy-Villacoublay, France) was used for modelling, and Ultimaker Cura 5.0.0 (Ultimaker, Zaltbommel, the Netherlands) was used for slicing and printing parameter setting (Table 2). Then, the samples were printed from horizontal (z = 4 mm) and vertical (z = 150 and 80 mm) directions through the Ultimaker2 printer (Ultimaker, Zaltbommel, the Netherlands). Ten samples were printed from each direction. Tensile and bending tests were undergone using the Zwick Roell Z005 (Zwick Roell, Herefordshire, the United Kingdom) at a constant strain rate of 2 mm/min until failure.

2.3. Scanning and modelling

The scanning data was obtained from a healthy 24-year-old female (163 cm, 55 kg). A DAVID 3D SCANNER 4.2.0.134 (David Vision Systems GmbH, Koblenz, Germany) was used for geometry capture. Before the scanning, the subject was asked to keep her left wrist in a pain-free functional position, and the wrist angle was controlled at 10-15° extension and 5-10° ulnar deviation using an arthrogoniometer [11,43]. Three retractable support components were used to assist the subject remain stationary (Fig. 3). Throughout the scanning, the scanner position was adjusted to obtain four scan segments from different perspectives (Fig. 3). Scanning a single segment took 2–5 s, and the entire

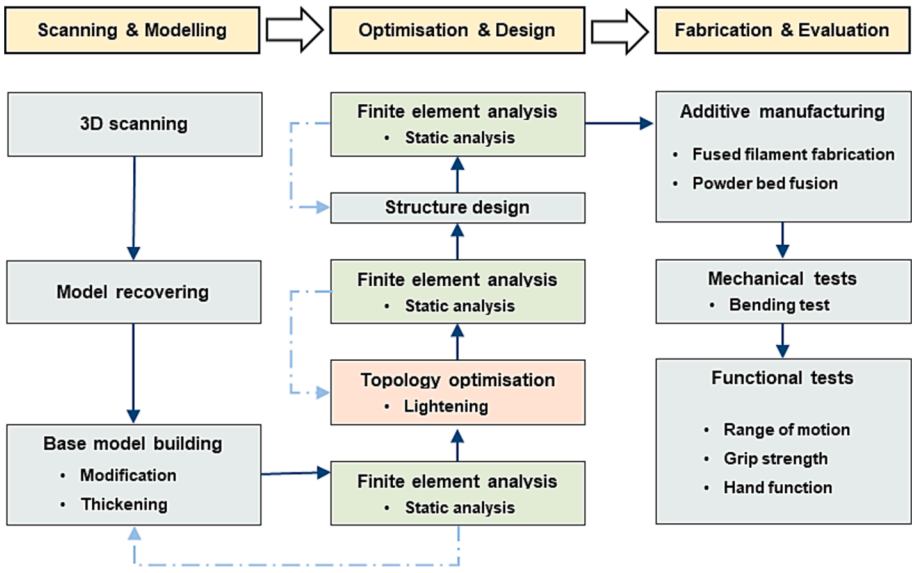

Fig. 1. The design and fabrication strategy based on AM and TO.

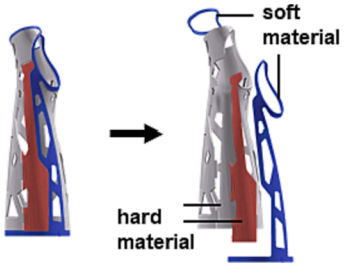

Splint	Hard material	Soft material
FFF Horizontal	PLA	resin
FFF Vertical	PLA	resin
PBF	PA2200	resin

Fig. 2. Materials selection for the designed splint.

Table 1
Material properties.

Material	PLA (horizontal)	PLA (vertical)	PA2200
Elastic modulus	2400 MPa	2210 MPa	1650 MPa
Poisson's ratio	0.35	0.35	0.38
Flexural Strength	92 MPa	43 MPa	58 MPa

Table 2
Printing parameters.

Parameters (Unit)	Value
Infill Density	100 %
Infill Pattern	cross
Nozzle Temperature (°C)	200

scanning process took 15 min. Then, the scanned elements were aligned and fused in the scanner software and exported as a polyhedron model (Fig. 3).

Geomagic Wrap 2021 (Geomagic, North Carolina, the United States) was used for model repair. Given the inevitable small movements of the limbs and the mutual covering between the fingers during scanning, the resulting body surface data may be rough and have holes. In this step, the restoration includes remeshing, noise reducing, hole filling, and surface smoothing. Besides, the thumb and finger parts were cursorily excised, as an RA splint does not need to cover them [44]. The repaired model was then proceeded to the exact surface partition, producing NURBS surface and exported as a surface model (Fig. 3).

Surface thickening and base model construction were done in SOLIDWORKS according to the wrist immobilisation splint section of the International Committee of the Red Cross (ICRC) published guidelines [44]. The splint length was set as one-third of the subject's upper limb, 223 mm. In order to minimise grip limitation [12], the part covering the proximal metacarpophalangeal joint was removed entirely. To increase comfort and to add padding between the splint and skin when required, the model was offset 1 mm outwards. To reduce compression on the swollen joint, the model was offset 1 mm outwards at the bony ramus (ulnar styloid process). In addition, the initial thickness of the splint was set as 1.8 mm [20,45], keeping the splint as light and thin as possible. The resulting solid model was then exported for FEA (Fig. 3).

2.4. Optimisation and design

To validate whether the prescribed initial thickness meets mechanical requirements, FEA was conducted using Ansys Workbench 19.0 (Ansys, Pennsylvania, the United States). A static structural module was created with the splint material defined as uniform linear elastic PA2200 (Table 1). The input model was meshed into 25,720 tetrahedral elements (2 mm size, 52,028 nodes). Convergence of the mesh was verified with a simulation difference of less than 2 % [46]. This static analysis simulated flexion and radial deviation motions of the wrist. A force of 120 N was applied in each direction, considered to exceed the extreme conditions achievable by RA patients [18]. The thickness set was assessed based on the obtained displacements, stress and safety factors. A higher safety factor indicates greater safety, with a safety factor less than 1.0 signifying material yielding.

The TO module was established based on the static analysis results, providing a theoretical reference for the splint lightweight design. The

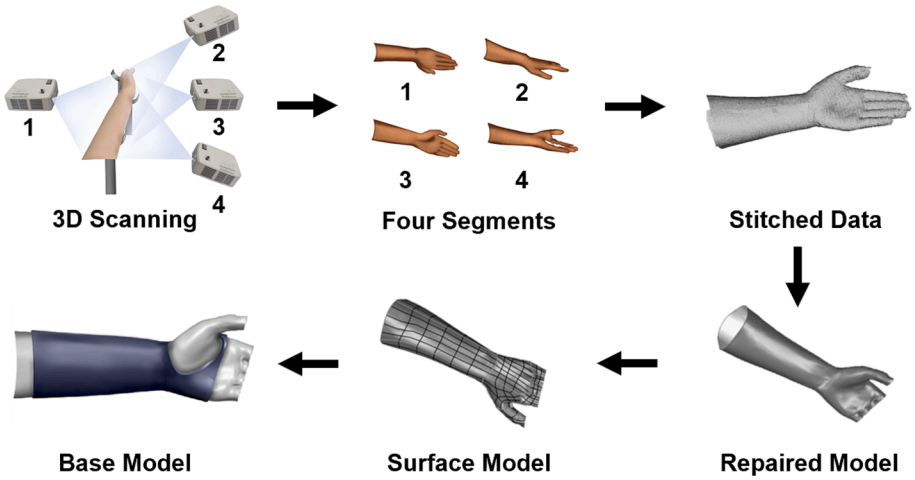

Fig. 3. Process of obtaining wrist surface data and creating the base model.

splint edges were defined as exclusion regions to ensure the structural integrity of the splint. Retained masses were set as 50 %, 55 %, and 60 %, with retention below 50 % excluded due to non-continuous structures. For each retention strategy, optimization results in two directions were combined through Boolean operations in Geomagic Wrap, getting the optimized models. These three optimized models were reimported into ANSYS and subjected to the aforementioned static simulations. An appropriate weight reduction strategy was determined based on the analysis results and discussions with orthotists. Guided by the chosen strategy, the base model was modified and separated into rigid and soft components, with the soft part serving as comfortable edging and connecting hinges.

Prior to manufacturing, FEA was used to validate the splint's mechanical performance and safety. Static analysis was conducted on the three designed splints for four motions: flexion, extension, radial deviation, and ulnar deviation. The input material properties are shown in Table 1. The simulated force applied is the maximum force achievable by RA patients. According to the perspective of Cazon et al., the force exerted by an RA patient's palm should not exceed 8 % of the maximum isometric force of a healthy individual [18]. By simplifying the forearm to a first-class lever, the calculated forces for flexion, extension, radial deviation, and ulnar deviation were 14.9 N, 8.4 N, 11.4 N, and 9.9 N, respectively. These forces are referred to as the 8 % load in subsequent sections. The validated models were then exported for 3D printing.

2.5. Fabrication

Three prototypes were fabricated in this study: an FFF horizontally printed splint (Z = frontal axis at anatomical position), an FFF vertically printed splint (Z = vertical axis at anatomical position), and a PBF printed splint.

The FFF splints were manufactured on Ultimaker2, and the PBF splint was fabricated on EOS Formiga P100 (EOS GmbH, Germany). Besides, the splints' flexible sections were fabricated through Polyjet on Stratasys J835 (Stratasys, Eden Prairie, the United States). The rigid and soft sections were joined by cyanoacrylate adhesive, which is only for research purposes and to demonstrate the complete composition of the splint. For the final product, the bonding between different materials can be chemical or mechanical [32].

2.6. Evaluation

Mechanical and functional tests were conducted on the obtained splint prototypes.

Bending tests were performed using a Zwick Roell Z0.5 testing machine (Zwick Roell, Herefordshire, the United Kingdom) under 14.9 N with a 4 mm/minute loading rate (Fig. 4A). Each splint was tested five times, outputting force–displacement curves, whose slope was calculated as the stiffness.

Support and loading modules were created for testing (Fig. 4A). For a valid comparison with FEA results, the shape of the contact surfaces was based on the splint's inner surface, matching the dimensions of the support and loading surfaces set in FEA. The modules were manufactured using Ultimaker2 with 45 % infill. Under 14.9 N loading, the module's deformation was less than 0.1 mm, which is not considered to affect test results.

Functional tests included ROM, grip strength, and hand function assessment.

Wrist ROM was measured with and without wearing the three splints (Fig. 4B). Without wearing splints, complete wrist mobility was measured in four directions: flexion, extension, radial deviation, and ulnar deviation. When wearing a splint, wrist angles in the resting position were additionally recorded. For angle monitoring, an inertial measurement unit (IMU) component (WitMotion, Shenzhen, China) was fixed to the distal dorsal aspect of the metacarpal, with ROM values displayed in its supporting software MiniIMU 6.2.68.0 (WitMotion, Shenzhen, China). Each test scenario was repeated five times.

During the measurement, given that the subject is a healthy individual, it is necessary to limit the subject's wrist strength to approximate the reality of RA patients. Therefore, a pressure sensor with a known resistance-force curve was used for force control. The sensor was placed between the skin and splint and connected to a multimeter, displaying the real-time resistance value. According to the meter reading, the force was controlled at the 8 % loading.

Grip evaluations were conducted with and without splints, recording the restricted grip strength and the position when achieving maximum grip strength (Fig. 4C). Grip strength was measured using a dynamometer, and the joint position was monitored using an IMU component. Each test scenario was repeated five times.

During the measurement, the participant's strength was not controlled for research purposes, as the relatively greater strength of healthy participants can magnify the splint's effect on the maximum grip strength and related posture.

As for hand function, the Jebsen-Taylor Hand Function Test was conducted with and without wearing splints (Fig. 4D). The original test comprised seven items. In this study, given that the test hand is non-dominant, the first item, handwriting, was reasonably omitted [47]. Each test scenario was repeated five times.

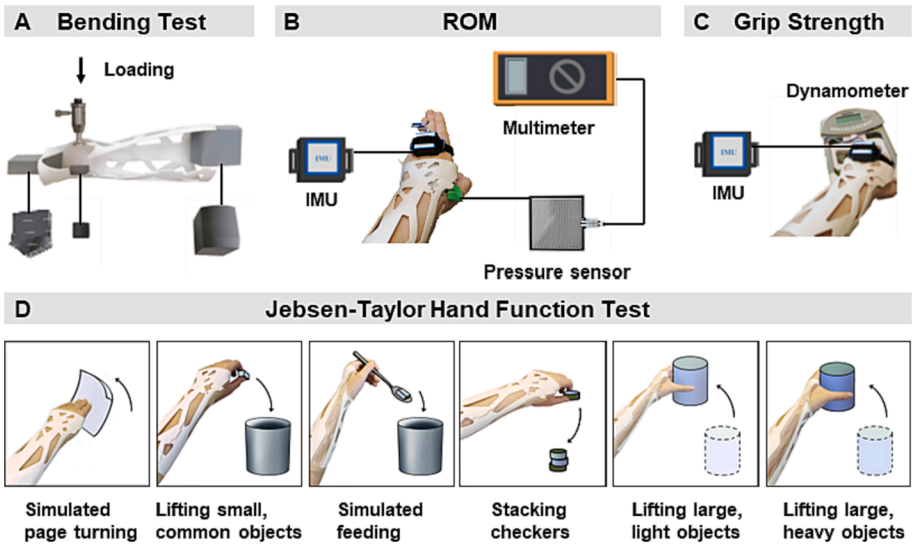

Fig. 4. Setup of the physical and functional tests. (A) Bending test and created modules. (B) Measurement of wrist ROM. (C) Measurement of grip strength. (D) Jebsen-Taylor hand function test.

3. Results

3.1. PLA elastic modulus

PLA standard samples and their force–displacement curves are shown in Fig. 5. Since the force applied to the splint in daily activities is similar to three-point bending, the bending modulus was chosen as the input value for FEA.

3.2. Optimisation and design results

FEA results for the base model are presented in Fig. 6A, confirming the adequacy of the set thickness. Safety factors in the flexion and radial deviation direction are 4.0 and 3.6, respectively, meeting safety requirements. The splint displacements also fulfil the functional needs of the splint, according to the consultation with experienced orthotists.

TO results are shown in Fig. 6A. Under 120 N loading, the optimized models derived from the three lightweight strategies do not reach their yield limit. The 50 % mass retention strategy is chosen in this study considering the breathability, lightweight, and structural design [16,17]. Additionally, as indicated in Fig. 6A, the structure on the radial side of the splint is optimised and removed, so the splint pockets and soft connections are designed in this position.

The final design based on TO is illustrated in Fig. 6B. The splint was designed as a single piece, featuring an opening for easy donning and doffing, which is crucial for patients with chronic degenerative conditions such as RA [15]. Also, a flexible linkage is designed for opening and closing, which can avoid using Velcro straps, and the splint edges are designed for soft contact.

Simulation results of the designed splint are shown in Table 3 and

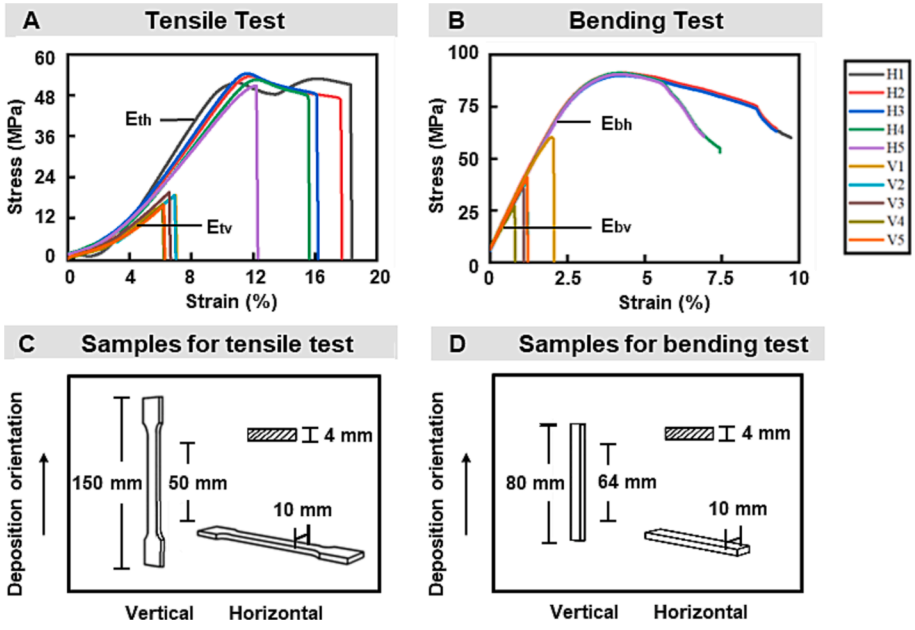

Fig. 5. Standard samples and their force–displacement curves. (A) Tensile testing, Eth = 1250 ± 55 Mpa = tensile modulus for horizontally printed samples, Etv = 840 ± 28 Mpa = tensile modulus for vertically printed samples. (B) Bending testing, Ebh = 2400 ± 23 MPa = bending modulus for horizontally printed samples, Ebv = 2210 ± 19 MPa = bending modulus for vertically printed samples. (C) Samples for tensile test. (D) Samples for bending test.

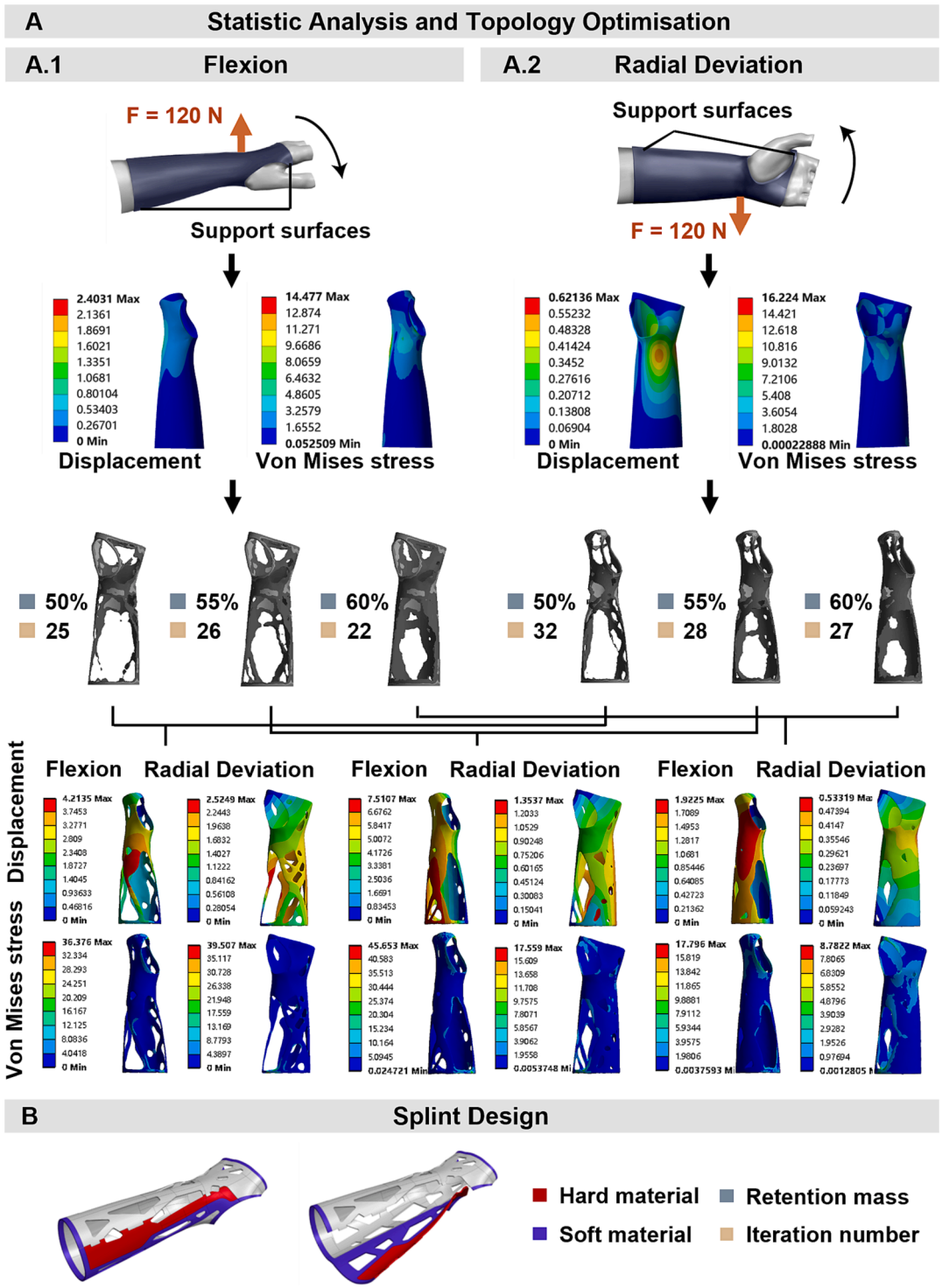

Fig. 6. (A) Optimisation in (A.1) flexion and (A.2) radial deviation, showing the boundary conditions, static analysis results and topology optimisation results. (B) Design of the splint showing open and closed states.

Table 3
Displacement simulations for the three splints at 8% load.

Movement	Load (N)	Max displacement in the main axes		
		FFF (horizontal)	FFF (vertical)	PBF
Flexion (-X)	14.9	1.6	1.7	2.2
Extension (X)	8.4	2.1	2.2	2.9
Radial deviation (-Z)	11.4	1.7	1.9	2.5
Ulnar deviation (Z)	9.9	2.2	2.4	3.2

Fig. 7. Safety factors of the PBF splint in flexion, extension, radial deviation, and ulnar deviation are 3.4, 6.0, 9.6, and 3.0, respectively, meeting the manufacturing requirements.

As shown in Table 3, the most significant excursions of the three splints occur in extension and ulnar deviation. The FFF horizontal splint is slightly stiffer than the vertical one, with the difference does not exceed 11.8 % in all four directions. In contrast, the PBF splint exhibits the maximum deformation, more than 29.4 % larger compared with FFF splints.

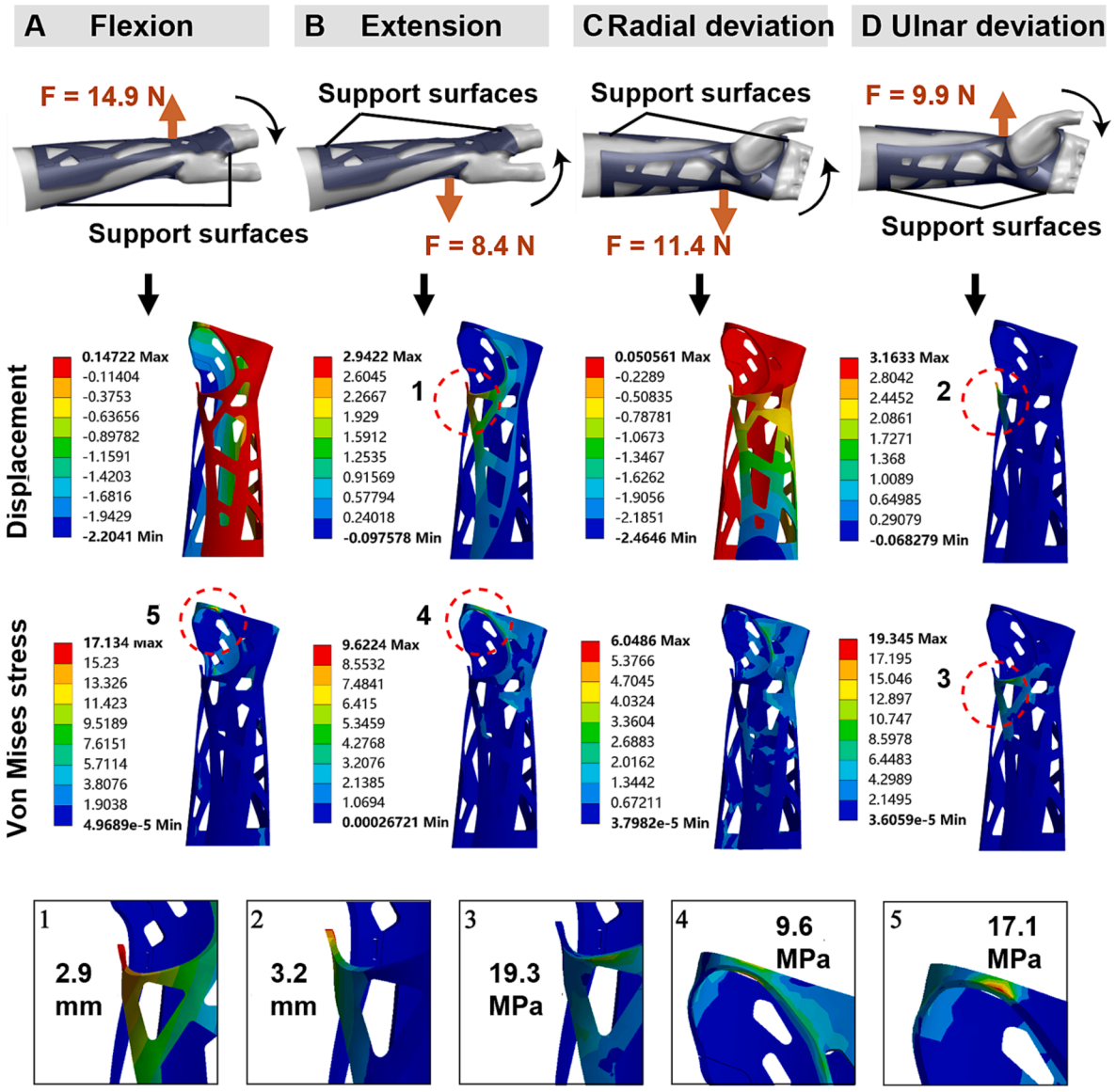

Fig. 7. The displacement and Von Mises stress results for the PA2200 splint in (A) flexion, (B) extension, (C) radial deviation, (D) ulnar deviation at 8% load.

According to the displacement and Von Mises stress results presented in Fig. 7, the maximum displacement happens in extension and ulnar deviation, concentrated at the projecting structure at the radial styloid. The maximum stress concentration (19.3 MPa) is also found in this structure, followed by the cross-bridge structure between the thumb and index finger, suggesting that the splint is relatively weak in these two areas.

3.3. Prototypes

Fabrication results are shown in Fig. 8. The longest manufacturing time is for FFF horizontal printing (36 h), and the shortest is for PBF (14 h), but PBF is the costliest (£95).

3.4. Evaluation results

As bending test results shown in Fig. 9, the stiffness of the FFF vertical splint is indicated as 6.5 % lower than that of the FFF horizontal splint. The stiffness of the PBF splint is 32.6 % lower than FFF horizontal splint and 27.9 % lower than FFF vertical splint. The displacements of FFF horizontal, FFF vertical and PBF splints are 2.9, 3.1, 4.8 mm, respectively.

The limited ROM is shown in Fig. 10A. Without the splint, the wrist ROM is 59.7° flexion, 51.6° extension, 25.0° radial deviation and 44.4° ulnar deviation. According to Fig. 10A, all three splints manage to meet the needs of RA patients in the resting position. During motions, the two FFF splints perform in general agreement and better than the PBF splint. In addition, the three splints are the least restrictive regarding ulnar deviation.

Grip evaluation results are shown in Fig. 10B.1, with 21.9 % of the full grip strength limited by the FFF horizontal splint, 18.7 % by the FFF vertical splint and 6.4 % by the PBF splint.

As shown in Fig. 10B.2, the maximum grip strength is reached at the extension and ulnar deviation posture. All three splints limit the ulnar deviation to less than 50 % of that without splints. However, the wrist extension angles are increased. This could imply a change in the force pattern: less ulnar deviation and more extension.

The impact of the splint on hand function is presented in Table 4. When wearing the splint, the completion times for all tasks increase, especially for “lifting large, heavy objects.” In addition, the completion times for “lifting large, light objects,” “simulated feeding,” and “simulated page turning” increase by more than 1s.

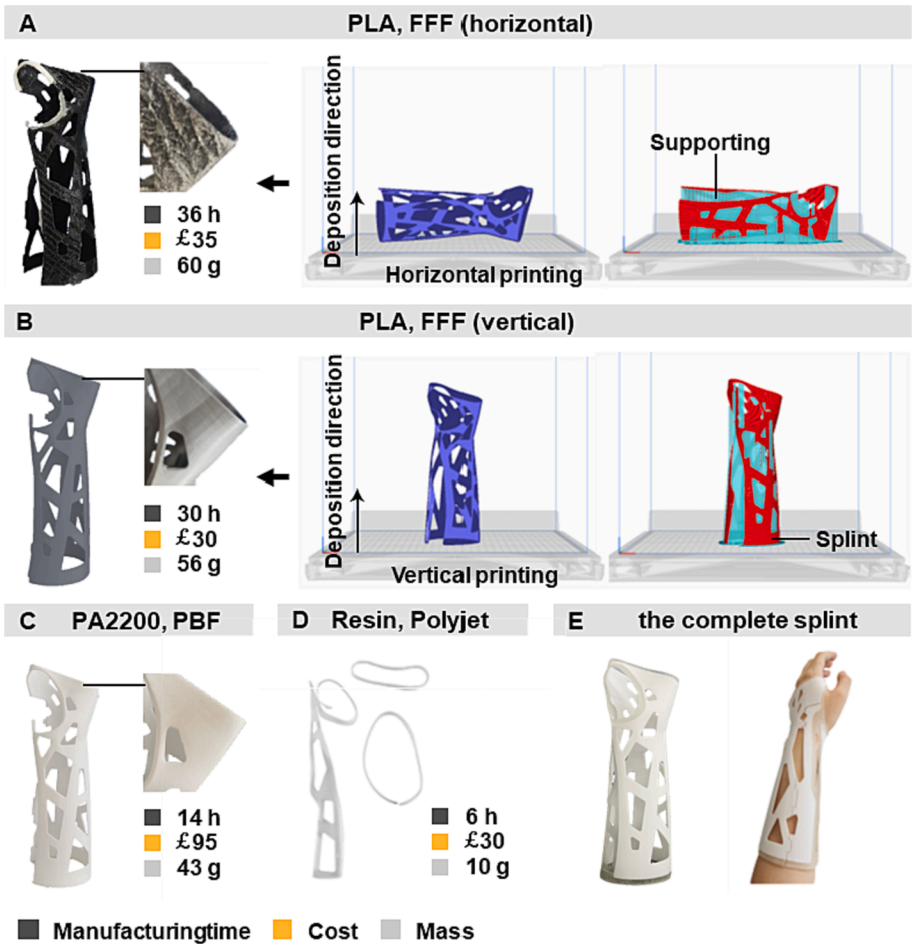

Fig. 8. Illustration of printed prototypes with their respective printing time, cost, and weight with (A) PLA, FFF (horizontal), (B) PLA, FFF (vertical), (C) PA2200, PBF, (D) Resin, Polyjet, (E) The complete splint. The printing directions and established supports for FDM are shown in (A) and (B).

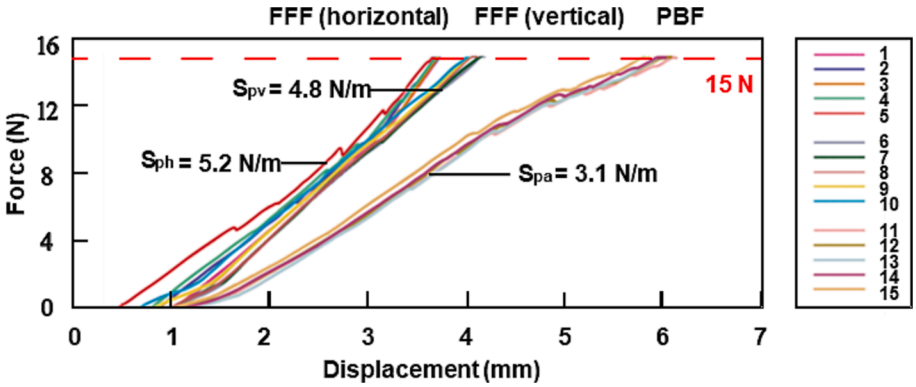

Fig. 9. Force-displacement curves of the three splints. Sph = stiffness for the FFF horizontal splint. Spv = stiffness for the FFF vertical splint. Spa = stiffness for the PBF splint.

The evaluation comparative results for the three splints are depicted in Fig. 11. Both FFF splints exhibit similarity in mechanical performance and functionality. The PBF splint retains the highest grip strength and exhibits the poorest hand function. In addition, the FFF vertical splint shows the highest total normalized value.

4. Discussion

As a recommended conservative treatment for RA, functional wrist splints are intended to immobilise the wrist joint in a pain-free position and provide support during movement [7,8,48]. AM combined with CAD allows for advanced customisation of RA splints [21,49]. However, the structural design of existing wrist splints, particularly concerning ventilation strategies, lacks theoretical foundation and biomechanical considerations [13,32,33,37]. Hence, in this study, a design and manufacturing process for customised wrist splints is proposed, with FEA and TO providing biomechanically based theoretical support. Based on the proposed strategy, three prototypes were produced using distinct AM methods and evaluated. The results demonstrate that the designed splints can meet the usage requirements of RA patients. In addition, FFF

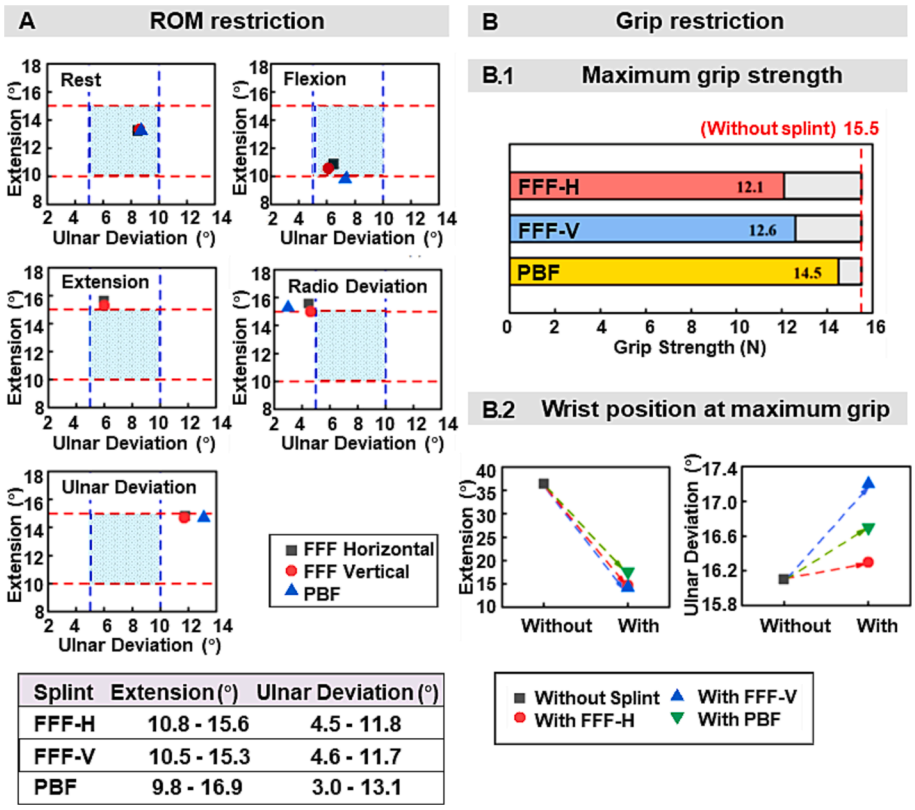

Splint	Extension (°)	Ulnar Deviation (°)
FFF-H	10.8 - 15.6	4.5 - 11.8
FFF-V	10.5 - 15.3	4.6 - 11.7
PBF	9.8 - 16.9	3.0 - 13.1

Fig. 10. (A) ROM restriction at rest and in motions. (B) (B.1) Maximum grip strength and (B.2) the relevant wrist position.

Table 4
Jebsen-Taylor Hand Function Test.

Items	Time spent to complete the items (s)			
	Without splint	FFF (horizontal)	FFF (vertical)	PBF
Simulated page turning	4.08	4.72 (+0.64)	4.63 (+0.55)	5.09 (+1.01)
Lifting small, common objects	3.75	4.13 (+0.38)	4.10 (+0.35)	4.07 (+0.32)
Simulated feeding	5.98	7.11 (+1.13)	6.90 (+0.92)	6.86 (+0.88)
Stacking checkers	4.05	4.73 (+0.68)	4.55 (+0.50)	5.02 (+0.93)
Lifting large, light objects	3.38	4.25 (+0.87)	4.43 (+1.05)	4.24 (+0.86)
Lifting large, heavy objects	3.73	4.55 (+1.18)	4.55 (+1.18)	4.54 (+1.17)
Total	24.97	29.49 (+4.52)	29.16 (+4.19)	29.82 (+4.85)

*Values in parentheses indicate the time taken while wearing the splint minus the time taken without wearing splints.

vertical printing is recommended for general clinical use, considering the splint's stiffness, functionality, surface quality, and cost.

The designed splints are verified from four aspects: mechanical performance, ROM limitation, grip strength retention, and hand function.

Regarding mechanical properties, all three splint prototypes have a safety factor greater than 3.0, which meets the manufacturing requirements. In addition, simulation (Table 3) and mechanical test results (Fig. 9) show that the designed splints do not fracture under the maximum force applied by RA patients, which meets the mechanical and safety needs. In terms of stiffness, the FFF horizontally printed splint displays a slight advantage over the vertically printed splint, with a difference of 6.5 %. This is not an unexpected result considering that the difference in bending modulus was 7.9 % between samples printed in the two orientations. At the same time, this may justify the choice of inputting bending modulus for FEA in this study. Another supporting reason is that the difference in tensile modulus between samples is 32.8 %, not corresponding to the difference between splints.

Functionally, the wrist ROM limitation provided by the developed splints meets the needs of RA patients. The designed splints limit 95.7 % sagittal movement and 89.8 % coronal movement. Similarly, Aranceta-Garza et al. compared ten commercially available wrist splints, with the best ROM limitation being 81.7 % sagittal movement and 90.4 % coronal movement (86.7 % flexion, 76.7 % extension, 97.3 % ulnar deviation, and 83.5 % radial deviation) [11]. However, in Aranceta-Garza et al.'s study, this restriction was not attributed to a single splint. In contrast, the designed splint in our study balances restrictions across all directional movements. In detail, at rest, all three splints can control the wrist in an expected position (10-15° extension and 5-10° ulnar deviation). While during motions, the wrist angles offset from the expected range. Given that the loads used for testing are the maximum forces achieved by RA patients, a small amount of angular excursion is acceptable. Nevertheless, when wearing the PBF splint, angle excesses occur in all directions of movement to varying degrees. This means that the current thickness of the PBF splint may not be sufficient. In addition, the three splints are the least restrictive for wrist ulnar deviation. This corresponds to the FEA results (Table 3), where the splint exhibits the maximum displacement in ulnar deviation. In conjunction with Fig. 7, this underperformance may be related to the projecting structure at the radial styloid, which is one of the structural weaknesses of the splint. One possible solution is partially thickening and widening this area to improve its stiffness. This treatment can also be applied to the cross-bridge structure between the thumb and index finger, another stress concentration area.

Concerning grip strength, the designed splints impose a limitation of 18.7 % on maximum grip strength, which is acceptable. In a study conducted by Aranceta-Garza et al. involving healthy people, the

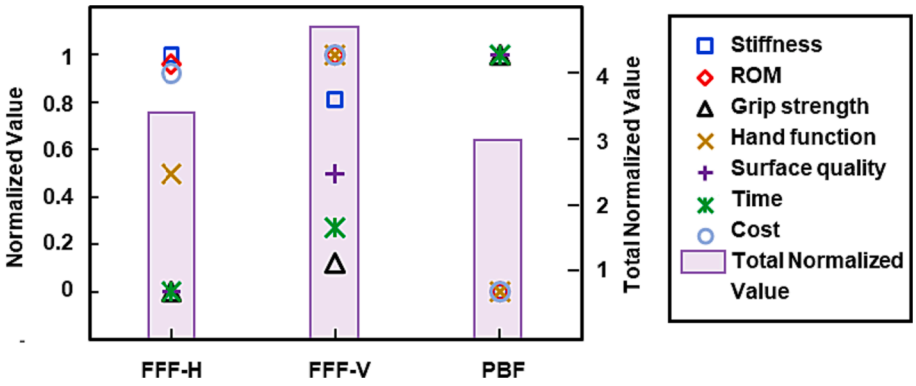

Fig. 11. Comparison of the three splints in terms of stiffness, ROM restriction, grip strength retention, hand function, surface quality, and cost.

minimum limitation was reported as 1.7 %, but this splint did not provide an appropriate ROM restriction [11]. In Sadura-Sieklucka et al.'s research on RA patients, grip limitations were found to be 60.6 % (right hand) and 58.4 % (left hand) compared to health controls [5]. Considering the inherent grip limitations associated with RA (40–67 %) [50,51], the observed 18.7 % limitation in our study is not anticipated to impede disease recovery. In healthy people, considering the constraints imposed by the splint on wrist extension and ulnar deviation, a decreased grip strength cannot be avoided [52,53]. Correspondingly, hand function also diminishes, particularly in tasks requiring strength, such as "lifting large, heavy objects," and those rely on agile wrist rotation like "simulated feeding" and "simulated page turning." However, the PBF splint, which retains the most grip strength, did not yield the best hand function (Fig. 11). This may be attributed to the fact that the retention of grip strength in the PBF splint is associated with softer material, which indicates less support and is not conducive to stabilizing the wrist during tasks. Further research is required to explore the splint trade-off between movement limitation, grip strength, and hand function. Additionally, wearing splints may affect the force pattern. In the present study, the extension angle was slightly greater after wearing splints. This may indicate that the subject attempted to achieve more grip strength through more significant extension due to the limitation of ulnar deviation. Aranceta-Garza et al. also reported the splint's effect on force pattern, but in their study, angles of both extension and ulnar deviation decreased [11]. This could be due to the different structures of dynamometers and splints between studies.

As for manufacturing, two manufacturing methods are involved in this study: FFF (two printing directions) and PBF. FFF is low-cost but with a compromised manufacturing accuracy [6]. Also, the anisotropy of FFF products may adversely limit achieving designed performance [42]. In contrast, PBF is expensive in equipment and materials but relatively accurate in manufacturing [54].

In order to explore the suitable manufacturing method for clinical application, three prototypes were compared, taking into account the safety (stiffness), functionality, surface quality, and cost. Fig. 11 shows that the FFF vertical splint has the maximum total normalized value among the three prototypes. Further elaboration is presented in the subsequent discussion.

Regarding safety, although the two FFF splints perform similarly in stiffness, the vertical splint is more prone to fracture. As shown in Fig. 5, vertical samples fracture like brittle materials, which is in accordance with previous studies [38,40]. Therefore, the vertical splint may suddenly fracture under a substantial impact to puncture the skin. Although it is unlikely that a patient with RA would achieve the force necessary to crack the splint, the possibility of a break under external force cannot be excluded. In contrast, horizontal samples not breaking under loading may imply a better safety profile for horizontally printed splints.

This potential fracture risk is related to the deposition direction. FFF products have composite structures where layers are stacked and bonded through heat and cooling processes [55]. Insufficient interlayer adhesion and air voids lead to anisotropy in the Z-axis direction [56]. Thus, FFF products are more prone to fracture under interlayer shear load [57], such as the vertically printed splint in this study. Our findings align with Casavola et al.'s experiments, which validated a decrease in the Young's modulus of FFF samples with an increasing grating angle [38]. The samples were easier to fracture at a grating angle of 90°, corresponding to our study's vertical printing angle. While various printing parameters, including speed and temperature, can impact the quality of FFF products, it is noteworthy that these parameters remained consistent in our FFF splints. Also, in the XY plane, both splints were filled with 100 % infill and orthogonal patterns, which mitigates the effect of infill on mechanical properties.

FFF splints show functional similarities (Fig. 11). However, the horizontal splint offers disadvantages in surface quality and cost. Due to the cylindrical structure of the splint, more support material is needed for horizontal printing. Removing the support material calls for special tools such as hand pliers, and polishing the surface requires additional time and effort [58]. A possible alternative method is using the water-soluble PVA material as support [29]. However, this would require special printing equipment and result in additional material consumption. In contrast, vertically printed splints require less manufacturing time and material consumption, reducing the price and shortening the delivery time.

PBF is a competitive choice if economic factors are not considered. Compared with FFF, PBF needs less manufacturing time and offers the best surface quality. In addition, PBF does not require extra support materials, meaning that the printed splint needs little post-processing [15]. Moreover, the PA2200 splint offers the best safety among the three splints, given the PBF's manufacturing characteristics, not relying on layering, and the properties of the nylon material itself [59].

Therefore, FFF vertical printing is recommended for common clinical use while considering using FFF horizontal printing in particular working environments with higher safety requirements. Besides, PBF is suitable for patients who do not care about the cost and want a high-quality splint as soon as possible. In accordance with findings from other existing papers, FFF fabrication with cost-effective and environmentally friendly PLA materials is currently the prevailing choice for 3D-printed medical appliances [60,61]. Walbran et al. conducted a comparative analysis of orthoses fabricated via FFF (PLA) and PBF (nylon) [62]. Their preference for the FFF one stemmed from its better mechanical properties (yield/fracture strain) and more economical cost. Conversely, Paterson et al. asserted that FFF is the least suitable process for AM splint fabrication compared to PBF, stereolithography (SLA) and Polyjet [13]. However, they only focused on the poor surface quality of FFF splints, omitting consideration of the functionality, cost, and the influence of FFF manufacturing parameters on product quality.

The difference between simulated and actual values is worth discussing. For FFF splints, the simulated value for displacement is around

55 % of the actual value. For the PBF splint, the simulated value is 46 % of the actual value. Although the difference between the simulated and actual values is significant, the two show a good correlation: the difference in displacement between the two FFF splints is small (simulated 6.3 %, actual 6.9 %), and the PBF splint shows the largest displacement.

The limitation of the simulation strategy in this study is one of the reasons for the discrepancy. For simplification purposes, the flexible part of the splint was deleted, ignoring its effect on mechanical properties. In addition, the gap between the rigid parts of the plywood was defined as fully bound, but in reality, there was micro-movement between them. Furthermore, some inputting material properties were from the manufacturer and did not take into account the influence of the manufacturing process.

Another reason is that the elasticity modulus of testing samples differs from that of the printed splint. Łukaszewski et al. found that the modulus of elasticity measured using standard samples was at least twice that of the splint, which is in line with the deformation difference in this study [23]. On the contrary, the experimental results of Cazon et al. reflect that the simulated value is about twice the actual value for the splint's displacement in wrist flexion [18]. However, given the differences in splint construction, materials, manufacturing methods, and force loading between Cazon et al.'s study and the present study, it is difficult to determine the reasons for the opposite results. Another notable point is that, according to Cazon et al.'s research, the difference between the simulated and actual values could vary in different force-loading directions [18]. They indicated a good correlation between the simulated and actual values at wrist extension and ulnar deviation, while the simulated value is nearly four times smaller than the actual value at radial deviation.

More research on the difference between FEA and physical test results for AM splints needs to be performed. According to Łukaszewski et al.'s experiments, for the simulation to be more realistic, the elastic modulus of the splints' mid-section structure could be measured for FEA [23]. However, since only ABS material was used in their study, it is unclear whether this conclusion can be generalised to other materials. In this study, the difference between simulated and actual values behaved differently in different materials (PLA and PA2200). However, given the different manufacturing processes between the two splints, it is hard to determine whether this variation is attributable to the material or the manufacturing process.

As for the limitations of this study, besides the simplification of FEA and reliance on data from manufacturers discussed above, other limitations are the small sample size and lack of clinical trials. Furthermore, the use of a non-movable scanner in this study extended the time required for body surface data collection, highlighting the potential advantages of employing a movable scanner [45]. In future studies, clinical research including RA patients will be considered to validate the feasibility and effectiveness of the proposed strategy. Also, the observed discrepancy between FEA and physical test results of AM splints deserves further investigation to improve the simulation accuracy.

5. Conclusion

This paper presents a design and manufacturing strategy for customized wrist splints, with the feasibility validated through different splint prototypes. The assessment results indicate that the designed splints meet the mechanical performance and functional requirements of RA patients. In FFF, the horizontally printed splint performed larger stiffness, but the deposition direction had a limited effect on the splint function. Furthermore, despite PBF offering superior splint surface quality and safety, FFF vertical printing is recommended as the most cost-effective printing method for general clinical use.

CRediT authorship contribution statement

Mo Zhou: Writing – review & editing, Writing – original draft, Visualization, Methodology, Investigation, Formal analysis, Data curation, Conceptualization. **Changning Sun:** Writing – review & editing, Visualization, Supervision. **Seyed Ataollah Naghavi:** Writing – review & editing, Visualization, Supervision. **Ling Wang:** Writing – review & editing, Supervision. **Maryam Tamaddon:** Writing – review & editing, Supervision. **Jinwu Wang:** Writing – review & editing, Supervision, Funding acquisition. **Chaozong Liu:** Writing – review & editing, Supervision, Funding acquisition, Conceptualization.

Declaration of competing interest

The authors declare that they have no known competing financial interests or personal relationships that could have appeared to influence the work reported in this paper.

Data availability

Data will be made available on request.

Acknowledgment

The authors would like to thank UCL Orthopaedic Research Group (University College London, UK) for the technical support in design and manufacturing of the devices.

Fundings

This paper was supported by Engineering and Physical Sciences Research Council via DTP CASE Programme (Grant No: EP/T517793/1); Royal Society via an International Exchange program (Grant No: IEC \NSFC\191253); and National Key R&D Program of China [Grant No: 2018YFE0207900].

References

[1] S.C. Higgins, J. Adams, R. Hughes, Measuring hand grip strength in rheumatoid arthritis, Rheumatol. Int. 38 (5) (2018) 707–714.
[2] W. Grassi, R. De Angelis, G. Lamanna, C. Cervini, The clinical features of rheumatoid arthritis, Eur. J. Radiol. 27 (1998) S18–S24.
[3] K. Trieb, Treatment of the Wrist in Rheumatoid Arthritis, J. Hand Surg. Am. 33 (1) (2008) 113–123.
[4] K. Ellegaard, C. von Bülow, A. Røpke, C. Bartholdy, I.S. Hansen, S. Rifbjerg-Madsen, M. Henriksen, E.E. Wæhrens, Hand exercise for women with rheumatoid arthritis and decreased hand function: an exploratory randomized controlled trial, Arthritis Res. Ther. 21 (1) (2019) 158.
[5] T. Sadura-Sieklucka, B. Sokołowska, A. Prusinowska, A. Trzaska, K. Księżopolska-Orłowska, Benefits of wrist splinting in patients with rheumatoid arthritis, Reumatologia 56 (6) (2018) 362–367.
[6] F. Górski, R. Wichniarek, W. Kuczko, M. Żukowska, M. Lulkiewicz, P. Zawadzki, Experimental studies on 3D printing of automatically designed customized wrist-hand orthoses, Materials 13 (18) (2020).
[7] S. Haskett, C. Backman, B. Porter, J. Goyert, G. Palejko, A crossover trial of custom-made and commercially available wrist splints in adults with inflammatory arthritis, Arthritis Care Res. 51 (5) (2004) 792–799.
[8] M.M. Veehof, E. Taal, M.J. Willems, M.A.F.J. van de Laar, Determinants of the use of wrist working splints in rheumatoid arthritis, Arthritis Rheum. 59 (4) (2008) 531–536.
[9] L. Ramsey, R.J. Winder, J.G. McVeigh, The effectiveness of working wrist splints in adults with rheumatoid arthritis: a mixed methods systematic review, J Rehabil Med 46 (6) (2014) 481–492.
[10] L. Deshaies, Arthrities, in: H.M. Pendleton, W. Schultz-Krohn (Eds.), Pedretti's occupational therapy : practice skills for physical dysfunction, Elsevier St. Louis, Missouri, St. Louis, Missouri, 2018, pp. 945–971.
[11] A. Aranceta-Garza, K. Ross, M. Buhler, E. Rameckers, A comparative study of efficacy and functionality of ten commercially available wrist-hand orthoses in healthy females: wrist range of motion and grip strength analysis, Frontiers in Rehabilitation Sciences 2 (2021) 687554.
[12] E. Fess, K. Gettle, C. Philips, R. Janson, Hand and Upper Extremity Splinting Principles & Methods, 3rd Edition,, 2005.
[13] A.M. Paterson, R. Bibb, R.I. Campbell, G. Bingham, Comparing additive manufacturing technologies for customised wrist splints, Rapid Prototyp. J. 21 (3) (2015) 230–243.
[14] D. Palousek, J. Rosicky, D. Koutny, P. Stoklásek, T. Navrat, Pilot study of the wrist orthosis design process, Rapid Prototyp. J. 20 (1) (2014) 27–32.

[15] S. Kelly A. Paterson R. Bibb A review of wrist splint designs for additive manufacture 2016 Loughborough University.
[16] X. Tan, W. Chen, J. Cao, S. Ahmed-Kristensen, A preliminary study to identify data needs for improving fit of hand and wrist orthosis using verbal protocol analysis, Ergonomics 64 (2) (2021) 259–272.
[17] M. Halanski, K.J. Noonan, Cast and Splint Immobilization: Complications, JAAOS - Journal of the American Academy of Orthopaedic Surgeons 16 (1) (2008).
[18] A. Cazon, S. Kelly, A.M. Paterson, R.J. Bibb, R.I. Campbell, Analysis and comparison of wrist splint designs using the finite element method: Multi-material three-dimensional printing compared to typical existing practice with thermoplastics, Proceedings of the Institution of Mechanical Engineers, Part H: Journal of Engineering in Medicine 231 (9) (2017) 881–897.
[19] G. Baronio, S. Harran, A. Signoroni, A critical analysis of a hand orthosis reverse engineering and 3D printing process, Appl. Bionics Biomech. 2016 (2016) 8347478.
[20] D.S. Chae, D.H. Kim, K.Y. Kang, D.Y. Kim, S.W. Park, S.J. Park, J.H. Kim, The functional effect of 3D-printing individualized orthosis for patients with peripheral nerve injuries: three case reports, Medicine (baltimore) 99 (16) (2020) e19791.
[21] G. Baronio, P. Volonghi, A. Signoroni, Concept and design of a 3D printed support to assist hand scanning for the realization of customized orthosis, Appl. Bionics Biomech. 2017 (2017) 8171520.
[22] T. Oud, Y. Kerkum, P. de Groot, H. Gijsbers, F. Nollet, M.A. Brehm, Production time and user satisfaction of 3-dimensional printed orthoses for chronic hand conditions compared with conventional orthoses: a prospective case series, J Rehabil Med Clin Commun 4 (2021) 1000048.
[23] K. Łukaszewski, R. Wichniarek, F. Górski, Determination of the elasticity modulus of additively manufactured wrist hand orthoses, Materials 13 (19) (2020).
[24] A.M.J. Paterson, R.J. Bibb, R.I. Campbell, A review of existing anatomical data capture methods to support the mass customisation of wrist splints, Virtual and Physical Prototyping 5 (4) (2010) 201–207.
[25] T.A.M. Oud, E. Lazzari, H.J.H. Gijsbers, M. Gobbo, F. Nollet, M.A. Brehm, Effectiveness of 3D-printed orthoses for traumatic and chronic hand conditions: a scoping review, PLoS One 16 (11) (2021) e0260271.
[26] T.-H. Huang, C.-K. Feng, Y.-W. Gung, M.-W. Tsai, C.-S. Chen, C.-L. Liu, Optimization design of thumbspica splint using finite element method, Med. Biol. Eng. Compu. 44 (12) (2006) 1105–1111.
[27] A. Zolfagharian, T.M. Gregory, M. Bodaghi, S. Gharaie, P. Fay, Patient-specific 3D-printed splint for mallet finger injury, International Journal of Bioprinting 6 (2) (2020).
[28] P. Reis, M. Volpini, J.P. Maia, I.B. Guimarães, C. Evelise, M. Monteiro, J.C. C. Rubio, Resting hand splint model from topology optimization to be produced by additive manufacturing, Rapid Prototyp. J. 28 (2) (2022) 216–225.
[29] W. Yan, M. Ding, B. Kong, X. Xi, M. Zhou, Lightweight splint design for individualized treatment of distal radius fracture, J. Med. Syst. 43 (8) (2019) 284.
[30] P. Lu, Z. Liao, Q. Zeng, H. Chen, W. Huang, Z. Liu, Y. Chen, J. Zhong, G. Huang, Customized three-dimensional-printed orthopedic close contact casts for the treatment of stable ankle fractures: finite element analysis and a pilot study, ACS Omega 6 (4) (2021) 3418–3426.
[31] Y.-C. Liao, C.-K. Feng, M.-W. Tsai, C.-S. Chen, C.-K. Cheng, Y.-C. Ou, Shape modification of the boston brace using a finite-element method with topology optimization, Spine 32 (26) (2007).
[32] D. Popescu, A. Zapciu, C. Tarba, D. Laptoiu, Fast production of customized three-dimensional-printed hand splints, Rapid Prototyp. J. 26 (1) (2020) 134–144.
[33] Y.J. Chen, H. Lin, X. Zhang, W. Huang, L. Shi, D. Wang, Application of 3D-printed and patient-specific cast for the treatment of distal radius fractures: initial experience, 3D, Print Med 3 (1) (2017) 11.
[34] J. Li, H. Tanaka, Rapid customization system for 3D-printed splint using programmable modeling technique – a practical approach, 3D, Printing in Medicine 4 (1) (2018) 5.
[35] Y.K. Modi, N. Khare, Patient-specific polyamide wrist splint using reverse engineering and selective laser sintering, Mater. Technol. 37 (2) (2022) 71–78.
[36] S. Trivedi, Finite element analysis: a boon to dentistry, J Oral Biol Craniofac Res 4 (3) (2014) 200–203.
[37] M. Formisano, L. Iuppariello, A. Casaburi, P. Guida, F. Clemente, An industrial oriented workflow for 3D printed, patient specific orthopedic cast, SN Applied Sciences 3 (11) (2021) 830.
[38] C. Casavola, A. Cazzato, V. Moramarco, C. Pappalettere, Orthotropic mechanical properties of fused deposition modelling parts described by classical laminate theory, Mater. Des. 90 (2016) 453–458.
[39] M.C. Faustini, R.R. Neptune, R.H. Crawford, S.J. Stanhope, Manufacture of passive dynamic ankle-foot orthoses using selective laser sintering, IEEE Trans. Biomed. Eng. 55 (2) (2008) 784–790.
[40] J.M. Chacón, M.A. Caminero, E. García-Plaza, P.J. Núñez, Additive manufacturing of PLA structures using fused deposition modelling: effect of process parameters on mechanical properties and their optimal selection, Mater. Des. 124 (2017) 143–157.
[41] M. Lay, N.L.N. Thajudin, Z.A.A. Hamid, A. Rusli, M.K. Abdullah, R.K. Shuib, Comparison of physical and mechanical properties of PLA, ABS and nylon 6 fabricated using fused deposition modeling and injection molding, Compos. B Eng. 176 (2019) 107341.
[42] G. Fang, T. Zhang, S. Zhong, X. Chen, Z. Zhong, C.C. Wang, Reinforced FDM: Multi-axis filament alignment with controlled anisotropic strength, ACM Trans. Graph. 39 (6) (2020) 1–15.
[43] E.W.-s. Tam, J. Yip, K.L. Yick, S.P. Ng, C. Fang, Investigation of Anatomical Shape of Thumb of de Quervain's Tenosynovitis Patients, in: R.S. Goonetilleke, S. Xiong, H. Kalkis, Z. Roja, W. Karwowski, A. Murata (Eds.) Advances in Physical, Social & Occupational Ergonomics, Springer International Publishing, Cham, 2021, pp. 346-352.
[44] Icrc, prp, Manufacturing Guidelines: Upper Limb Orthoses (Physical Rehabilitation Programme) 2014 Geneva, Switzerland.
[45] S.J. Kim, S.J. Kim, Y.H. Cha, K.H. Lee, J.-Y. Kwon, Effect of personalized wrist orthosis for wrist pain with three-dimensional scanning and printing technique: a preliminary, randomized, controlled, open-label study, Prosthet. Orthot. Int. 42 (6) (2018) 636–643.
[46] A. Zolfagharian, T.M. Gregory, M. Bodaghi, S. Gharaie, P. Fay, Patient-specific 3D-printed Splint for Mallet Finger Injury, Int J Bioprint 6 (2) (2020) 259.
[47] E.D. Sears, K.C. Chung, Validity and responsiveness of the Jebsen-Taylor Hand Function Test, J. Hand Surg. Am. 35 (1) (2010) 30–37.
[48] G. Ward, A. Thompson, R. Squire, Hand and wrist orthoses for adults with rheumatological conditions. Practice guidelines for occupational therapists, (Second Edition),, Royal College of Occupational Therapists, London, 2020.
[49] J. Lee, A. Huang, Fatigue analysis of FDM materials, Rapid Prototyping Journal 19 (4) (2013) 291–299.
[50] M. Drużbicki, J. Zwolińska, G. Przysada, M. Maj, Assessment of hand mobility in patients with rheumatoid arthritis using a computer measurement station, Reumatologia/rheumatology 51 (2) (2013) 133–138.
[51] M. Woźniewski, A. Skrzek, H. Sabir, Z. Zagrobelny, Hand and knee function after systemic cryotherapy and exercises in patients with rheumatoid arthritis, Reumatologia 39 (2001) 155–163.
[52] S.W. O'Driscoll, E. Horii, R. Ness, T.D. Cahalan, R.R. Richards, K.N. An, The relationship between wrist position, grasp size, and grip strength, J Hand Surg Am 17 (1) (1992) 169–177.
[53] J.-A.-M. Lee, S.M. Sechachalam, The effect of wrist position on grip endurance and grip strength, The Journal of Hand Surgery (american Ed.) 41 (10) (2016) e367–e373.
[54] B. Yao, Z. Li, F. Zhu, Effect of powder recycling on anisotropic tensile properties of selective laser sintered PA2200 polyamide, Eur. Polym. J. 141 (2020) 110093.
[55] S.H. Ahn, M. Montero, D. Odell, S. Roundy, P.K. Wright, Anisotropic material properties of fused deposition modeling ABS, Rapid Prototyp. J. 8 (4) (2002) 248–257.
[56] N. Zohdi, R. Yang, Material anisotropy in additively manufactured polymers and polymer composites: a review, Polymers 13 (19) (2021) 3368.
[57] M.H. Sehhat, A. Mahdianikhotbesara, F. Yadegari, Verification of stress transformation in anisotropic material additively manufactured by fused deposition modeling (FDM), Int. J. Adv. Manuf. Technol. 123 (5) (2022) 1777–1783.
[58] Y.H. Cha, K.H. Lee, H.J. Ryu, I.W. Joo, A. Seo, D.H. Kim, S.J. Kim, Ankle-Foot orthosis made by 3D printing technique and automated design software, Appl. Bionics Biomech. 2017 (2017) 9610468.
[59] L. Waldburger, R. Schaller, C. Furthmüller, L. Schrepfer, D.J. Schaefer, A. Kaempfen, 3D-Printed hand splints versus thermoplastic splints: a randomized controlled pilot feasibility trial, Int J Bioprint 8 (1) (2022) 474.
[60] Y.J. Choo, M. Boudier-Revéret, M.C. Chang, 3D printing technology applied to orthosis manufacturing: narrative review, Annals of Palliative Medicine 9 (6) (2020) 4262–4270.
[61] A. Demeco, R. Foresti, A. Frizziero, N. Daracchi, F. Renzi, M. Rovellini, A. Salerno, C. Martini, L. Pelizzari, C. Costantino, The upper limb orthosis in the rehabilitation of stroke patients: the role of 3D printing, Bioengineering 10 (11) (2023) 1256.
[62] M. Walbran, K. Turner, A.J. McDaid, Customized 3D printed ankle-foot orthosis with adaptable carbon fibre composite spring joint, Cogent Engineering 3 (1) (2016) 1227022.